ISSN 1063-7850, Technical Physics Letters, 2018, Vol. 44, No. 7, pp. 650–653. © Pleiades Publishing, Ltd., 2018.
Original Russian Text © N.V. Artyukhova, Yu.F. Yasenchuk, A.S. Garin, V.E. Gyunter, 2018, published in Pis'ma v Zhurnal Tekhnicheskoi Fiziki, 2018, Vol. 44, No. 14, pp. 103–110.

Influence of Cobalt and Molybdenum Additives on the Structure and Shape Memory Parameters of Reaction-Sintered Porous Nickel Titanium Alloys

N. V. Artyukhova[a]*, Yu. F. Yasenchuk[a], A. S. Garin[a], and V. E. Gyunter[a]

[a] *Tomsk State University, Tomsk, 634050 Russia*

**e-mail: artyukhova_nad@mail.ru*

Received September 27, 2017

Abstract—We have studied the structure and properties of porous nickel titanium (TiNi) alloys obtained upon reaction sintering of Ti and Ni powders with Co and Mo additives. It is established that Co and Mo doping additives retain the compaction of Ni powder achieved at the initial stage of sintering. The maximum deformation of porous samples loaded in the austenite state was observed upon adding Co, while the addition of Mo resulted in minimum deformation. The addition of Co leads to single-stage martensitic transformation in TiNi phase, while the addition of Mo leads to the two-stage transformation that is more homogeneous over the volume. Both Co and Mo additives lead to increase in the maximum accumulated strain due to the formation of favorably oriented stress-induced martensite and reoriented quench-induced martensite.

DOI: 10.1134/S1063785018070192

The properties of monolithic nickel titanium (TiNi) alloys can be effectively controlled by varying the content of nickel in the TiNi phase in a concentration interval of 48–51.5 at % [1]. In reaction-sintered porous TiNi alloys, a much more pronounced effect can be achieved using various doping additives. In addition, the process of reaction sintering (RS) as controlling factor is a part of the combined method of obtaining TiNi-based implants. Therefore, it was important to consider the influence of doping on the structure and properties of Ti–Ni system in more detail. The choice of Co and Mo as doping additives was related to the fact that cobalt is closest to Ni in properties and forms a series of intermetallic compounds with Ti, while molybdenum does not react with Ti and only forms a continuous series of solid Mo–Ti solutions [1]. Thus, the mechanisms of influence of Mo and Co doping additives on the properties of TiNi-based alloys act in opposite directions, which can help to establish specific features of these factors.

The RS of Ti–Ni system alloys is stimulated by melting of the Ti_2Ni phase in the vicinity of 1223 K. However, a necessary condition for the sintering of high-porosity alloys is a small amount of liquid phase, which prevents their shrinkage and retains a regular porous structure. On the other hand, this circumstance hinders mass transport in a sintered system [2] and leads to unavoidable inhomogeneity of its phase composition.

The present work was aimed at studying the structure and properties of porous permeable $Ti_{50}Ni_{49}Co_1$, $Ti_{50}Ni_{49}Mo_1$, and $Ti_{50}Ni_{50}$ alloys prepared from powdered nickel (PNK-OT4 grade), titanium (PTEM grade), cobalt (PK-1u grade), and molybdenum (MPCh grade) components. The average particle dimensions were 10–15 μm for Ni and 60–80 μm for Ti. Cylindrical samples with dimensions of 48 × 8 mm of TiNi alloys containing 1 at % Co, 1 at % Mo, and additive-free composition were prepared by method of RS in quartz tubes at 1223 K for 5.4×10^3 s. The RS temperature for $Ti_{50}Ni_{50}$ alloy was selected so as to obey the condition of retaining regular porous structure and shape of samples. Based on the phase diagram of Ti–Ni system [1, 2], the maximum RS temperature was restricted to 1223 K and the minimum RS temperature was set as corresponding to the appearance of low-temperature eutectic liquid (near 1213 K). The optimum temperature–time RS regime selected for the $Ti_{50}Ni_{50}$ system was also used for the RS of Ti_{50}–Ni_{49}–Co_1 and Ti_{50}–Ni_{49}–Mo_1 alloy systems.

Specific features of martensitic transformations and macrodeformation characteristics were studied using multiply repeated shape memory effect (MSME) measurements under constant load (6×10^{-2} kgf) conditions of bending for porous plates with 35 × 7 × 1-mm dimensions. The optimum load was selected so that 1- to 2-mm bending of a sample plate in the austenite

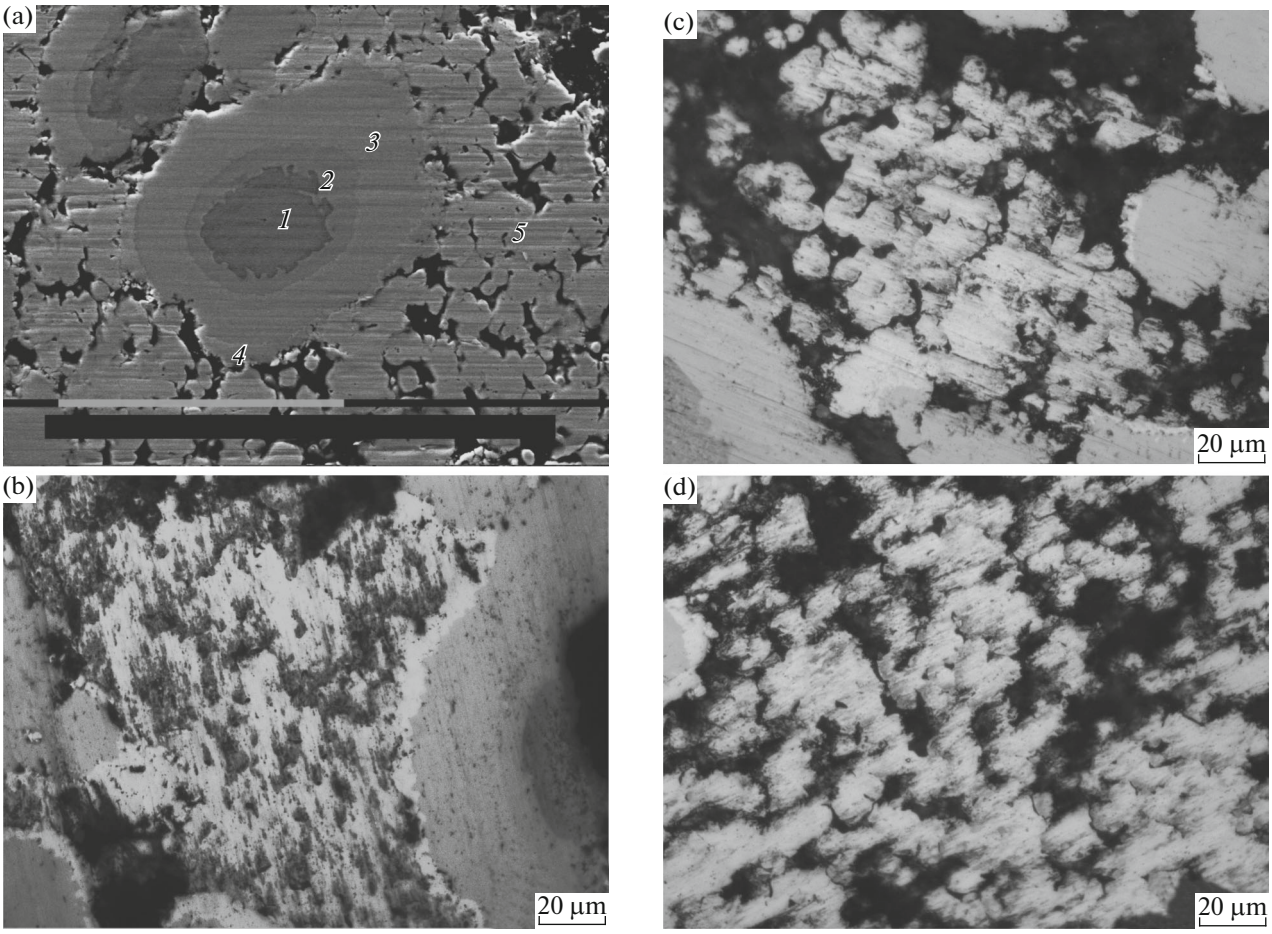

Fig. 1. SEM images showing (a) phase composition of a reaction cell in the solid-state RS stage (including (*1*) Ti_β, (*2*) Ti_2Ni, (*3*) TiNi, (*4*) $TiNi_3$, and (*5*) Ni_γ) [3] and (b–c) spongy nickel matrix in porous (b) $Ti_{50}Ni_{50}$, (c) $Ti_{50}Ni_{49}Co_1$, and (d) $Ti_{50}Ni_{49}Mo_1$ alloys.

state would not leave any residual strain upon unloading.

The structure of porous samples was studied using an Axiovert 25 Mat optical microscope and scanning electron microscopy (SEM) using a Philips SEM 515 instrument. The elemental composition of phases was determined by energy-dispersive X-ray (EDX) spectroscopy on an EDAX ECON IV electron-probe microanalyzer. Quantitative analysis of the sintering process was based on the measurement and description of distances between centers of particles in the central and peripheral zones of samples.

The phase structure of porous $Ti_{50}Ni_{50}$ alloy is well differentiated and can be considered as a set of reaction cells (see Fig. 1a), each cell comprising Ti_β core *1*, spongy Ni_γ matrix *5* at the periphery, and shells of Ti_2Ni *2*, TiNi *3*, and $TiNi_3$ *4* phases around the core [2, 3]. Investigation of the structural features and deformation behavior of porous samples revealed two reaction-cell components, TiNi and Ni_γ, which significantly influence the MSME parameters. This behavior is related to the fact that the TiNi phase exhibits the shape memory effect (SME), while Ni_γ occupies the main volume fraction of the alloy and influences the mechanical behavior of the sample.

Upon doping, the alloy structure remains generally the same, the reaction cells are retained, and TiNi phase is visually unchanged, but the spongy Ni_γ matrix exhibits visible changes. In ternary $Ti_{50}Ni_{49}Co_1$ and $Ti_{50}Ni_{49}Mo_1$ alloys, the spongy matrix has the form of a restricted solid solution of Ni_γ with Co and Mo additives, respectively. Note that the small content of doping additives hinders their observation by means of EDX microanalysis.

The entire sintered volume of porous $Ti_{50}Ni_{50}$ can be separated into two zones: central and peripheral. The spongy matrix in the central zone is noticeably denser (Fig. 1b) than in the peripheral zone (Fig. 1a), which is related to a temperature difference between these zones. The heat of the exothermal reaction between reactants provides additional heat supply to the system. However, heat removal via the peripheral

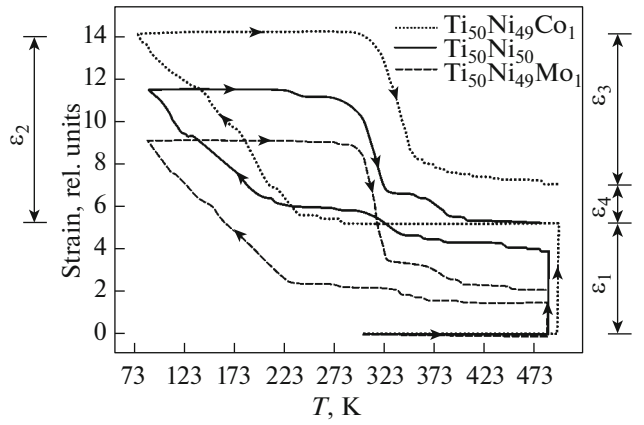

Fig. 2. Temperature dependences of macrodeformation $\varepsilon(T)$ in TiNi-based alloys $Ti_{50}Ni_{50}$, $Ti_{50}Ni_{49}Co_1$, and $Ti_{50}Ni_{49}Mo_1$.

zone accounts for the higher temperature in the central zone and lower temperature at the periphery.

An increased density of the spongy matrix is quantitatively manifested by reduced distances between centers of nickel particles. In the central zone of the $Ti_{50}Ni_{50}$ sample, the average value of this distance is about 7 μm, while that in the peripheral zone is about 11 μm. In the alloys doped with Co and Mo, these average values at the periphery differ rather insignificantly (8 versus 9 μm, respectively), while those in the central zone are the same (8 μm in both cases). Visible differences between $Ti_{50}Ni_{49}Co_1$ and $Ti_{50}Ni_{49}Mo_1$ alloys are related to retarded process of densification of the spongy matrix at the solid-state RS stage (cf. Figs. 1c, 1d), which hinders the growth of contact interfaces between nickel particles and limits the diffusion mass transfer during sintering. An increase in the activation energy of nickel self-diffusion in the presence of molybdenum and its decrease under the action of cobalt were also reported in [4, 5].

The doping additives of Co and Mo similarly influenced the densification behavior and morphology of nickel-based matrix, but differently affected the mechanical properties of TiNi phase. Observations revealed a relationship between the structure and MSME parameters of porous samples studied. Some of the temperature dependences of macrodeformation $\varepsilon(T)$ related to the cooling and heating under load reflect the behavior of strained TiNi phase (Fig. 2). The straining under load in the high-temperature state (ε_1) reflects the total contribution of TiNi phase deformation corresponding to stress-induced martensite formation and the plastic deformation of the Ni_γ matrix. The contribution from the spongy matrix is greater due to its volume fraction exceeding those from other parts of the reaction cell. The deformation of this phase depends on its porosity and the plasticity of nickel particles.

The maximum deformation under load in the austenite state (ε_1) is observed for $Ti_{50}Ni_{49}Co_1$ alloy (Fig. 2). In view of the influence of a spongy matrix of the reaction cell, this is probably related to its increased porosity, retained plasticity upon doping, and, hence, higher deformability of this alloy. In the $Ti_{50}Ni_{49}Mo_1$ alloy sample, the value of this type of deformation is 2.5 times smaller than in $Ti_{50}Ni_{50}$. Therefore, doping with Mo reduced the plasticity of nickel as compared to that in the undoped $Ti_{50}Ni_{50}$. We believe that this behavior is due to strengthening of the spongy matrix based on Ni particles via the mechanism of dispersion hardening [1]. Indeed, the reaction diffusion of Mo into the spongy nickel matrix probably leads to the formation of a finely dispersed intermetallic Mo–Ni phase, which accounts for hardening of the Ni_γ solid solution.

In $Ti_{50}Ni_{49}Co_1$ alloy, the direct phase transformation begins without a clearly pronounced region usually attributed to the $B2 \leftrightarrow R$ transition, which makes the martensitic transformation almost single-stage (Fig. 2). However, part of this dependence (related to the growth of a martensite phase) differs from rectilinear and displays several steps on the growth stage. We believe that this character of $\varepsilon(T)$ curve reflects a mixed type of the phase transformation, combining the formation of R-phase nuclei (on troughs) and the subsequent nucleation and growth of martensite crystals (on steep portions). Evidently, this order of transitions is related to nonuniform loading of the porous system and the chemical and structural inhomogeneity of the TiNi phase. Note that the two stages of martensitic transformation are clearly separated on the $\varepsilon(T)$ curve.

The $B2 \leftrightarrow R$ and $R \leftrightarrow B19$ transitions in $Ti_{50}Ni_{49}Co_1$ alloy under load are well pronounced, although poorly identified on the temperature dependence of the electric resistance of samples [6]. Therefore, external loading effectively favors the growth of R-phase and martensite, which is related to the process of monodomain structure formation [1]. It can be suggested that Co impurity in TiNi phase stimulates this process so that the growth of a martensite phase becomes more consistent and, hence, the accumulated strain (ε_2) in this sample becomes maximum (Fig. 2). Another factor that increases deformation in the direction of loading (ε_2) is an increase in the level of intrinsic stresses in austenite under the action of cobalt [6], which hinders reversibility of the martensitic transformation under the action of a bending load (ε_3) and, in turn, increases the residual strain (ε_4). The doping additive of molybdenum only influences the residual strain, the magnitude of which is reduced by 30% relative to that in the initial $Ti_{50}Ni_{50}$ alloy.

The martensite start temperature in all alloys studied varies in the interval of 243–203 K, the reverse transition onset temperatures are also close in all three

cases, and the rates of these processes are comparable. The values of temperature hysteresis in $Ti_{50}Ni_{50}$ and $Ti_{50}Ni_{49}Mo_1$ alloys are comparable (419 and 422 K, respectively, for $R \leftrightarrow B19'$ transition) and reach 467 K in $Ti_{50}Ni_{50}Co_1$ alloy.

In concluding, Co and Mo additives retard densification of the spongy Ni_γ-based matrix at the solid-state RS stage, thus limiting the diffusion mass transport in the Ti–Ni system. The Co additive retains plasticity and porosity of the spongy matrix and leads to an increase in the magnitude of deformation in a sample loaded in the austenite state (ε_1). In contrast, the Mo additive decreases this value by strengthening the nickel matric at the initial RS stage. Additionally, Co additive provides an increase in the maximum accumulated strain (ε_2) in TiNi phase as a result of the formation of oriented stress-induced martensite and re-oriented quench-induced martensite. This additive also makes the martensitic transformation close to single-stage, whereas the transformation in Mo-doped alloy is two-stage and more homogeneous over the volume.

Acknowledgments. This investigation of the structure of porous TiNi alloys was supported in the framework of a state order from the Ministry of Education and Science of the Russian Federation, project no. 3.6492.2017/6.7 VU (2018). Features of the martensitic transformations in TiNi alloys were studied in the framework of the Program of Increasing the Competitiveness of the Tomsk State University, project no. 8.8.23.2018.

REFERENCES

1. G. A. Baigonakova, E. S. Marchenko, and V. E. Gyunter, Tech. Phys. Lett. **43**, 940 (2017).
2. M. Whitney, S. F. Corbin, and R. B. Gorbet, Acta Mater. **56**, 559 (2007).
3. N. V. Artyukhova, Yu. F. Yasenchuk, and V. E. Gyunter, Russ. J. Non-Ferrous Met. **54**, 178 (2013).
4. A. A. Vasilyev, S. F. Sokolov, N. G. Kolbasnikov, and D. F. Sokolov, Phys. Solid State **53**, 2194 (2011).
5. Yu. A. Shchepochkina, RF Patent No. 2321652, Byull. Izobret. No. 10 (2008).
6. Yu. F. Yasenchuk, N. V. Artyukhova, V. E. Gyunter, and J.-S. Kim, Tech. Phys. Lett. **41**, 894 (2015).

Translated by P. Pozdeev